

RESEARCH ARTICLE | JULY 06 2023

Kinetic study of ion acoustic waves in Venusian ionosphere

T. Kamalam   ; S. V. Singh  ; T. Sreeraj  ; G. S. Lakhina 

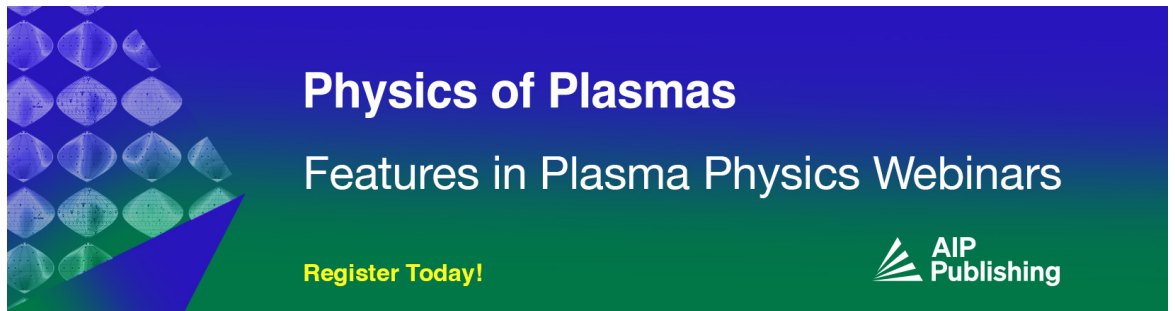


Physics of Plasmas 30, 072901 (2023)

<https://doi.org/10.1063/5.0145486>




CrossMark



Physics of Plasmas
Features in Plasma Physics Webinars

Register Today!



Kinetic study of ion acoustic waves in Venusian ionosphere

Cite as: Phys. Plasmas **30**, 072901 (2023); doi: 10.1063/5.0145486

Submitted: 6 February 2023 · Accepted: 13 June 2023 ·

Published Online: 6 July 2023



View Online



Export Citation



CrossMark

T. Kamalam,^{1,a)} S. V. Singh,² T. Sreeraj,² and G. S. Lakhina²

AFFILIATIONS

¹School of Physics and Astronomy, University of Southampton, Southampton SO17 1BJ, United Kingdom

²Indian Institute of Geomagnetism, Navi Mumbai 410218, India

^{a)}Author to whom correspondence should be addressed: kt2c22@soton.ac.uk

ABSTRACT

Kinetic dispersion of the ion acoustic waves has been explored for an unmagnetized five component plasma system comprising of Venusian protons, Venusian oxygen ions, Venusian electrons, solar wind protons, and kappa electrons. The solar wind protons and electrons are assumed to be streaming along the ambient magnetic field. The plasma parameters for this study have been obtained from Lundin *et al.* [Icarus **215**(2), 751–758 (2011)] for the dawn dusk meridian of Venus Express with the data from the ASPERA-4 ion mass analyzer. Our analysis revealed that two modes, viz., ion acoustic mode and beam driven mode, are excited for the considered plasma parameters. The ion acoustic mode exists due to the Venusian ions, and its growth rate is influenced by the solar wind beam electrons. The beam driven mode's existence and its growth rate depend on the solar wind beam protons. We conjecture that the ion acoustic mode and the beam driven mode could be useful in explaining the electrostatic noise in the Venusian ionosphere in the range of several hundreds Hz to 1 kHz and several tens kHz, respectively.

© 2023 Author(s). All article content, except where otherwise noted, is licensed under a Creative Commons Attribution (CC BY) license (<http://creativecommons.org/licenses/by/4.0/>). <https://doi.org/10.1063/5.0145486>

I. INTRODUCTION

Earth's sister planet Venus is eminently different when it comes to the intrinsic magnetic field. Venus has an induced magnetosphere but no intrinsic magnetosphere unlike our Earth. When solar wind interacts with Venus's atmosphere, ionization occurs, which gives rise to the ionosphere, and the movement of ionized particles in the ionosphere produces electric currents. These electric currents, in turn, create the magnetic field, which shields the planet from solar wind. This induced magnetic field slows and deflects solar wind around Venus. However, the induced magnetosphere is not so strong, resulting in the comet-like atmosphere erosion process, also known as ionospheric losses (ion escape) in Venus. The interaction between solar wind and Venus produces different types of fluctuation in Venus's ionosphere and the magnetosphere, which can be interpreted via plasma waves. These waves play a vital role in altering the particle distribution function and accelerating the particles to high energy. In addition to these, plasma waves are responsible for the particle pickup process, dissipation, and energy transfer.¹

Venus is one of the most explored planets in the solar system. Various space missions assigned to Venus have provided extensive amounts of data. In addition, several spacecraft such as Solar Orbiter,²

Parker Solar Probe,³ etc., furnished data when they flew by Venus during their gravity assist maneuver. Among different spacecraft, the Pioneer Venus Orbiter (PVO) was the first one that could detect plasma wave activity.⁴ Various plasma waves have been observed in Venus, such as ion acoustic waves (IAWs),⁵ Langmuir waves,⁶ whistler waves,⁷ lower hybrid waves,⁸ proton cyclotron waves,⁹ and mirror mode waves.¹⁰ The review paper of Yadav¹ discusses the observation of the plasma waves around Venus and Mars in detail. Recently, Hadid *et al.*¹¹ analyzed the plasma properties of Venus's magnetosphere via Solar Orbiter and found various electromagnetic and electrostatic wave modes, such as ion acoustic waves, whistler waves, and Langmuir waves, and also solitary structures in the magnetosheath of Venus. One of the prominent low frequency plasma waves in the Venusian environment is ion acoustic waves. These prevalent IAWs have been observed in various regions in the Venusian environment, such as in the upstream bow shock region,^{12,13} ionopause region,⁵ and ionosheath region.¹⁴ These IAWs are believed to be generated via either the interaction of the neutral Venus atmosphere with the upstream solar wind or due to the ion acceleration at the planetary shock front. Moreover, it has been proposed that the energy from solar wind to Venus's ionosphere can be transferred via ion acoustic waves.¹⁵

Apart from observations, IAWs have been investigated for some theoretical studies also. The most recent theoretical analysis of IAW in the Venusian induced magnetosphere is carried out by Sayed *et al.*,¹⁶ wherein the Korteweg–de Vries (KdV) equation and Sagdeev pseudo-potential methods are employed for the investigation. They investigated the nonlinear IAWs for an unmagnetized multicomponent plasma consisting of Venusian O⁺ and H⁺ ions and electrons with Maxwellian distribution. They compared their theoretical analysis with the observations of Venus Explorer (VEX) in the noon midnight meridian. For this study, they have used the parameters from Lundin *et al.*¹⁷ Recently, Fayad *et al.*¹⁸ carried out the linear analysis of obliquely propagating low frequency electrostatic waves for a plasma system comprising of Venusian O⁺ and H⁺ ions and electrons obeying Maxwellian distribution. Their linear dispersion relation predicted the excitation of two plasma modes, viz., modified ion acoustic mode and drift mode for their plasma system. Moslem *et al.*¹⁹ analyzed the IAWs in a multi fluid plasma model by using the Gardner equation. Salem *et al.*²⁰ investigated losses from the ionosphere of Venus to the solar wind for a plasma system comprising of Venusian protons, Venusian Oxygen, solar wind electrons, and protons. They found that for noon midnight meridian data, the oxygen ion to electron relative density may be the significant factor to enhance the ionic loss. The nonlinear electrostatic structures in Venus’ ionospheric plasma have been investigated by Elmandoh *et al.*,²¹ and their results revealed that Venus’s ionosphere supports both subsonic and supersonic compressive ion acoustic waves.^{1,11} The electrostatic solitary waves in Venus’s ionosphere were recently studied by Rubia *et al.*²² Their results could be useful in interpreting the Pioneer Venus Orbiter’s observed electrostatic waves in the frequency range of 100 Hz to 5.4 kHz in Venus’s ionosphere.

Extensive literature review shows that most of the theoretical investigations of the ion acoustic waves in Venus have been carried out using nonlinear methods and some via linear fluid method. Using nonlinear methods, one can get all the necessary information regarding the potential profile and the electric field profile of the nonlinear plasma waves. In the linear fluid method, one can study the dispersion characteristics of the plasma waves. However, the microscopic processes involved in the plasma such as the growth of the wave modes, wave-particle interactions, the Landau damping, or the trapping of the charged particles can only be studied using the kinetic theory. The kinetic study of ion acoustic waves on Venus has not been explored so far, which motivated us to pursue this current work. Theoretical investigation via kinetic dispersion relation could provide complementary information about the generation and nature of the ion acoustic waves and the plasma properties in the induced magnetosphere of Venus.

II. THEORETICAL MODEL

We have considered homogenous, collisionless, unmagnetized Venusian plasma comprising of Venusian oxygen ions O⁺, Venusian protons H⁺ ions, Venusian electrons, streaming solar wind protons, and electrons. The solar wind beam electrons are assumed to obey the Kappa distribution.²³ The electron distribution function in the solar wind consists of three components, namely, lower energy core electrons, higher energy halo electrons, and a higher energy magnetic field aligned strahl.²⁴ In the case of the slow solar wind, the electron distribution function is often characterized by the core and halo electrons,

whereas in the case of the fast solar wind, strahl electron is also observed along with the core and halo electrons. In our study, we have not considered the strahl electrons as its number density is usually low in comparison with the core and halo electrons. Observations by Ulysses²⁵ and Cluster²⁶ showed that the electron velocity distribution function in the solar wind can be modeled well with kappa distribution. The kappa distribution considered here represents the total electron distribution, i.e., it describes both the core and suprathermal electrons components of the solar wind. We have considered Maxwellian distribution for the remaining four components.

The kinetic dispersion relation for the electrostatic waves in such a plasma system can be written as^{23,27}

$$1 + \frac{2\omega_{vp}^2}{k^2\theta_{vp}^2} [1 + \xi_{vp}Z(\xi_{vp})] + \frac{2\omega_{vo}^2}{k^2\theta_{vo}^2} [1 + \xi_{vo}Z(\xi_{vo})] + \frac{2\omega_{sp}^2}{k^2\theta_{sp}^2} [1 + \xi_{sp}Z(\xi_{sp})] + \frac{2\omega_{se}^2}{k^2\theta_{se}^2} \left[1 - \frac{1}{2\kappa} + \xi_{se}Z(\xi_{se})\right] + \frac{2\omega_{ve}^2}{k^2\theta_{ve}^2} [1 + \xi_{ve}Z(\xi_{ve})] = 0, \tag{1}$$

where *vp* (*vo*) denotes Venusian protons (oxygen), *sp* represents solar wind beam protons, *se* is the solar wind beam electrons, and *ve* represents Venusian electrons. Also, $Z(\xi)$ is the plasma dispersion function.²⁸

The argument of the plasma dispersion function, ξ_j , is given by the following expression:

$$\xi_j = \frac{\omega - ku_j}{k\theta_j}. \tag{2}$$

Here, *j* corresponds to individual plasma species, ω is the wave frequency, and *k* is the wave number. We have considered the beam velocity $u_j=0$ for Venusian proton, oxygen, and electron ($j = vp, vo, \text{ and } ve$, respectively); thermal velocity for Maxwellian distribution is given as $\theta_j = \sqrt{\frac{2k_B T_j}{m_j}}$, with $j = vp, vo, sp, \text{ and } ve$, and thermal velocity for Kappa distribution is $\theta_{se} = \sqrt{\frac{2\kappa-3}{\kappa} \frac{k_B T_{se}}{m_{se}}}$.

Furthermore, $\omega_j = \sqrt{\frac{N_j e^2}{\epsilon_0 m_j}}$ is the plasma frequency of the *j*th species.

We have considered the large argument limit for ions, which is as follows:

$$\xi_{vp}, \xi_{vo}, \xi_{sp} \gg 1. \tag{3}$$

We have considered the small argument limit for electrons,

$$\xi_{se}, \xi_{ve} \ll 1. \tag{4}$$

The limit $\xi \ll 1$ represents the phase velocity of the wave is less than that of the thermal velocity of the particular plasma component, and $\xi \gg 1$ represents the case where the phase velocity of the wave is higher than the thermal velocity of the particular plasma component. To get ion acoustic waves, thermal velocity of electrons should be greater than the wave’s phase velocity, so we have considered $\xi \ll 1$ for both electrons, and the thermal velocity of ions should be less than the wave’s phase velocity, so we have considered $\xi \gg 1$ for all ions in our system.

The plasma dispersion function for the Maxwell Boltzmann distribution function is as follows:²³

$$Z(\xi) = -2\xi + \frac{4}{3}\xi^3 + i\sqrt{\pi}e^{-\xi^2} \quad \xi \ll 1, \quad (5)$$

$$Z(\xi) = -\frac{1}{\xi} - \frac{1}{2\xi^3} - \frac{3}{4\xi^5} + i\sqrt{\pi}e^{-\xi^2} \quad \xi \gg 1. \quad (6)$$

The expansion for the Kappa distribution is²³

$$Z_\kappa(\xi) = \frac{\kappa! \sqrt{\pi} i}{\kappa^{3/2} \Gamma(\kappa - 1/2)} \left[1 - \left(\frac{\kappa + 1}{\kappa} \right) \xi^2 \right] - \frac{(2\kappa - 1)(2\kappa + 1)}{2\kappa^2} \xi \left[1 - \left(\frac{2\kappa + 3}{3\kappa} \right) \xi^2 \right] \quad \xi \ll 1. \quad (7)$$

We have ignored the real part contribution for the electrons. Substituting the imaginary part of Eq. (5) and real and imaginary parts of Eq. (6), and substituting the first order imaginary part in Eq. (7) in Eq. (1) give

$$\begin{aligned} & 1 + \frac{2\omega_{vp}^2}{k^2 \theta_{vp}^2} \left[-\frac{1}{2\xi_{vp}^2} - \frac{3}{4\xi_{vp}^4} + i\sqrt{\pi}e^{-\xi_{vp}^2} \right] \\ & + \frac{2\omega_{vo}^2}{k^2 \theta_{vo}^2} \left[-\frac{1}{2\xi_{vo}^2} - \frac{3}{4\xi_{vo}^4} + i\sqrt{\pi}e^{-\xi_{vo}^2} \right] \\ & + \frac{2\omega_{sp}^2}{k^2 \theta_{sp}^2} \left[-\frac{1}{2\xi_{sp}^2} - \frac{3}{4\xi_{sp}^4} + i\sqrt{\pi}e^{-\xi_{sp}^2} \right] \\ & + \frac{2\omega_{se}^2}{k^2 \theta_{se}^2} \left[\frac{2\kappa - 1}{2\kappa} + \xi_{se} \frac{\kappa! \sqrt{\pi} i}{\kappa^{3/2} \Gamma(\kappa - \frac{1}{2})} \right] \\ & + \frac{2\omega_{ve}^2}{k^2 \theta_{ve}^2} \left[1 + \xi_{ve} i\sqrt{\pi}e^{-\xi_{ve}^2} \right] = 0. \end{aligned} \quad (8)$$

Substituting Eq. (2) in the aforementioned equation, the real part of the aforementioned equation gives

$$D_r = 1 - \frac{\omega_{vp}^2}{\omega^2} - \frac{\omega_{vo}^2}{\omega^2} - \frac{\omega_{sp}^2}{(\omega - ku_{sp})^2} + \frac{2\omega_{se}^2}{k^2 \theta_{se}^2} \left[\frac{2\kappa - 1}{2\kappa} \right] + \frac{2\omega_{ve}^2}{k^2 \theta_{ve}^2}. \quad (9)$$

We get the same dispersion relation for both fluid and kinetic description. However, from the fluid dispersion relation, one cannot analyze the resonant wave growth as it provides only the non-resonant wave growth information, whereas the kinetic dispersion relation allows us to study the resonant wave growth.

The corresponding derivative of the real part is

$$\frac{dD_r}{d\omega} = \frac{2\omega_{vp}^2}{\omega^3} + \frac{2\omega_{vo}^2}{\omega^3} + \frac{2\omega_{sp}^2}{(\omega - ku_{sp})^3}. \quad (10)$$

The imaginary part is as follows:

$$\begin{aligned} D_i &= \frac{2\omega_{vp}^2}{k^2 \theta_{vp}^2} \left(\frac{\omega}{k\theta_{vp}} \right) \sqrt{\pi}e^{-\xi_{vp}^2} + \frac{2\omega_{vo}^2}{k^2 \theta_{vo}^2} \left(\frac{\omega}{k\theta_{vo}} \right) \sqrt{\pi}e^{-\xi_{vo}^2} \\ &+ \frac{2\omega_{sp}^2}{k^2 \theta_{sp}^2} \left(\frac{\omega - ku_{sp}}{k\theta_{sp}} \right) \sqrt{\pi}e^{-\xi_{sp}^2} + \frac{2\omega_{se}^2}{k^2 \theta_{se}^2} \left(\frac{\omega - ku_{se}}{k\theta_{se}} \right) \\ &\times \left[\frac{\kappa! \sqrt{\pi}}{\kappa^{3/2} \Gamma(\kappa - \frac{1}{2})} \right] + \frac{2\omega_{ve}^2}{k^2 \theta_{ve}^2} \left(\frac{\omega}{k\theta_{ve}} \right) \sqrt{\pi}e^{-\xi_{ve}^2}. \end{aligned} \quad (11)$$

Now, considering $\omega = \omega_r + i\gamma$ with $\gamma/\omega_r \ll 1$, the real frequency ω_r can be obtained from the solution of $D_r = 0$. Then, γ can be obtained from the following relation:

$$\gamma = -\frac{D_i}{dD_r/d\omega}. \quad (12)$$

$$\gamma = -\frac{D_i}{\frac{2\omega_{vp}^2}{\omega^3} + \frac{2\omega_{vo}^2}{\omega^3} + \frac{2\omega_{sp}^2}{(\omega - ku_{sp})^3}}. \quad (13)$$

In Sec. III, numerical analysis of the dispersion relation has been carried out.

III. NUMERICAL RESULTS

For our plasma model, an extensive parametric study has been conducted for the observed data from Lundin *et al.*¹⁷ for the dawn dusk meridian of Venus Express (VEX) with the data from the ASPERA-4 Ion Mass Analyzer (IMA). The plasma parameters for our study are obtained from the ionospheric region at altitude 200–1000 km. The unnormalized and normalized plasma parameters used in this study are given in Table I. For our numerical analysis, the following normalizations have been used: all number densities are normalized by the equilibrium plasma density N_0 , time by the proton plasma frequency $\omega_{pi} = \sqrt{\frac{N_0 e^2}{\epsilon_0 m_p}}$, distance by the solar wind beam electron Debye length $\lambda_{De} = \sqrt{\frac{\epsilon_0 k_B T_{se}}{N_0 e^2}}$, and velocity by the ion acoustic wave velocity $C_a = \sqrt{\frac{k_B T_{se}}{m_p}}$. In this manuscript, we have denoted the normalized beam velocity as U_j , where j stands for sp and se . The normalized parameters at 1000 km altitude are as follows: number density of Venusian protons $N_{vp} = 0.4$, number density of Venusian Oxygen $N_{vo} = 0.5$, number density of solar wind beam protons, number density of solar wind beam electrons $N_{sp} = N_{se} = 0.1$, and number density of the Venusian electrons $N_{ve} = 0.9$. From Fig. 9 in Lundin *et al.*,¹⁷ we have obtained the solar wind proton number density. Since we have considered only solar wind protons and not any other solar wind component, we have obtained the solar wind electron number density from the assumption that number density of solar wind electrons and protons are equal. The temperature ratio of Venusian protons to the solar wind beam electrons and the temperature ratio of Venusian Oxygen to the solar wind beam electrons are $\sigma_{vp} = \sigma_{vo} = 0.003$, the temperature ratio of solar wind protons to solar wind beam electrons

TABLE I. The unnormalized number density for dawn dusk meridian obtained from Lundin *et al.*¹⁷ The last three columns in this table show the normalized number densities. The normalized number densities are calculated as $N_j = \frac{n_j}{n_0}$, where $j = sp, vo, \text{ and } vp$.

L (kms)	n_{sp} (cm ⁻³)	n_{vo} (cm ⁻³)	n_{vp} (cm ⁻³)	$n_0 = n_{sp} + n_{vo} + n_{vp}$	N_{sp}	N_{vo}	N_{vp}
1000	10	50	40	100	0.1	0.5	0.4
800	8.5	50	40	98.5	0.08	0.51	0.41
600	6	100	28	134	0.04	0.75	0.21
400	3.5	180	15	198.5	0.01	0.91	0.08

is $\sigma_{sp} = 0.001$, and the temperature ratio of Venusian electrons to the solar wind beam electrons is $\sigma_{ve} = 0.45$.^{16,19} The beam velocity of solar wind protons and solar wind electrons is $U_{sp} = U_{se} = 9.84$, and the suprathermal index is $\kappa = 2$. In general, solar wind electron distributions can be fitted well with kappa values from 1.5 to 7. The fast solar wind electrons distribution from Ulysses observations at distance 1.35–1.5 AU is shown to have approximately $\kappa = 2$ (Table I in Livadiotis²⁰). We have considered $\kappa = 2$ for our study, which corresponds to the furthest state from thermal equilibrium. The plasma parameters were chosen according to the ζ condition in Eqs. (3) and (4). For the parameters considered in our plasma system, all the conditions on ζ are satisfied.

The total charge neutrality condition for the normalized number densities is as follows:

$$N_{vp} + N_{vo} + N_{sp} = N_{se} + N_{ve} = 1. \quad (14)$$

The charge neutrality condition for the normalized number densities of the solar wind particles is

$$N_{sp} = N_{se}. \quad (15)$$

We have obtained four modes [highest power of ω in real part of the dispersion relation D_r in Eq. (9) is 4] in the system, viz., one ion acoustic mode, two positive beam modes with positive phase velocity, and

one ion acoustic mode with negative phase velocity. We got three roots with positive phase velocity in our plasma system but only two roots, one having low frequency and another high frequency, have positive growth rates as shown in Figs. 1(a) and 1(b), respectively. The low frequency mode dispersion curve is plotted in Fig. 1(a), and its corresponding growth rate is plotted in Fig. 1(c). The high frequency mode has been plotted in Fig. 1(b), and its corresponding growth rate has been plotted in Fig. 1(d).

Figure 1(a) highlights that the low frequency mode shows the typical ion acoustic dispersion trend. For $k\lambda_{De} = 3$, the corresponding frequency of this mode is 0.586. We have normalized frequency ω with respect to the proton plasma frequency ω_{pi} , and the ideal ion acoustic wave mode should possess frequency $\omega < \omega_{pi}$. The low frequency mode $\omega/\omega_{pi} < 1$ throughout their variation, which indicates that it is, indeed, ion acoustic wave mode. The high frequency wave mode in Fig. 1(b) exhibits linear trend, and its frequency $\omega/\omega_{pi} > 1$ and goes up to 29.80 for $k\lambda_{De} = 3$. The high frequency mode could not be an ideal ion acoustic wave mode, since ion acoustic wave mode satisfies $\omega < \omega_{pi}$ where ω_{pi} is the ion plasma frequency. A quick calculation of ω/k , i.e., $29.80/3$, gives us 9.93, which is comparable with the normalized solar wind beam proton flow velocity $U_{sp} = 9.84$ in our model. This signifies that the high frequency wave mode is driven by the contribution of the beam components. It is clear from Eq. (9) that the high frequency mode comes from the contribution of the solar

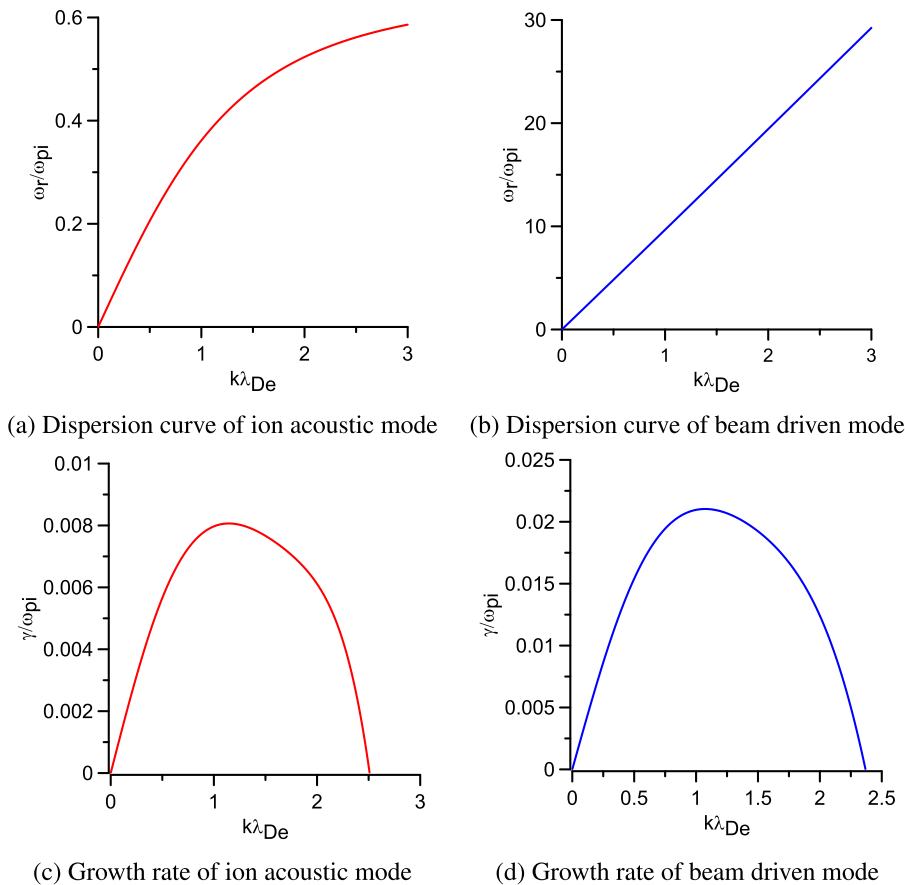


FIG. 1. The dispersion characteristics for the considered plasma system at 1000 km altitude. The plasma parameters are as follows: $N_{vp} = 0.4$, $N_{vo} = 0.5$, $N_{sp} = N_{se} = 0.1$, $N_{ve} = 0.9$, $\sigma_{vp} = \sigma_{vo} = 0.003$, $\sigma_{sp} = 0.001$, $\sigma_{ve} = 0.45$, $U_{sp} = U_{se} = 9.84$, and $\kappa = 2$.

wind beam protons. Therefore, we conclude that the existence of high frequency wave mode arises as a result of the solar wind beam protons contribution.

The corresponding growth rate of the dispersion relation of Figs. 1(a) and 1(b) is plotted in Figs. 1(c) and 1(d). The beam driven mode [Fig. 1(d)] growth rate increases initially, reaches maximum $\gamma/\omega_{pi} = 0.0210$ at $k\lambda_{De} = 1.073$, and gradually decreases. The similar trend has been observed for the low frequency mode [Fig. 1(c)], and it increases and reaches maximum $\gamma/\omega_{pi} = 0.0081$ at $k\lambda_{De} = 1.145$ followed by gradual decrease. We have obtained some broad idea about the wave modes, but mode analysis might extend the explanations on the role of each components and its impact on the instability of the wave modes.

Extensive mode analysis shows that whenever the number density of the solar wind beam electrons (N_{se}) or the beam velocity of the solar wind electrons (U_{se}) is zero, the low frequency ion acoustic mode excitation is no more possible, i.e., no positive γ . This suggests that the low frequency ion acoustic mode is excited by the solar wind beam electrons. Following the similar trait, we have deduced that whenever one of the following parameters N_{sp} (number density of solar wind beam protons), U_{sp} (beam velocity of solar wind beam protons) or N_{ve} (number density of Venusian electrons) becomes zero, the high frequency beam driven mode vanishes. The idea that solar wind beam protons could excite the beam driven mode is comprehensible because instabilities develop when there is a source of free energy available in the system. The beam ions or electrons could act as a source of energy for generating the instabilities. Therefore, one can deduce that the solar wind beam protons are required to generate the instability for the beam driven mode. However, it is not so clear that why Venusian electrons are needed for the instability of the beam driven mode. The Venusian electrons do not possess any energy source to provide for the wave mode generation. However, we have observed that, in the absence of Venusian electrons (N_{ve}), there is no wave growth for the beam driven mode. In usual case, the denominator of γ is positive, so the imaginary part of any component with the higher magnitude and with the negative sign contributes to the instability.

Here, the denominator of γ became negative, i.e., $\frac{2\omega_{vp}^2}{\omega^3} + \frac{2\omega_{vo}^2}{\omega^3} + \frac{2\omega_{sp}^2}{(\omega - ku_{sp})^3} < 0$. For our current parameter set, the beam velocity of the solar wind protons is higher than that of the phase velocity, i.e., $u_{sp} > V_{phase} = \frac{\omega_r}{k}$, which, in turn, makes the denominator of Eq. (13) negative; therefore, the imaginary part of any component with higher magnitude and with positive sign contributes to the instability (positive γ) for a wave mode. For the beam driven mode, the main contribution seems to come from the Venusian electrons. We have found that the beam mode satisfies the following condition $\frac{u_{sp}}{1 + \frac{N_{sp}}{N_{ve}}^{1/3}} < v_p < u_{sp}$, where $N_{vi} = N_{vp} + m_{po}N_{vo}$, $m_{po} = m_p/m_o$ is the mass ratio of the protons to the oxygen ions and $v_p = \frac{\omega}{k}$ is the phase velocity of the wave. Mathematically, the growth of the beam driven mode depends on the Venusian electrons. However, we strongly believe that the source for the growth of beam driven mode originates from the beam velocity of the solar wind protons. The reason is that Venusian electrons do not possess any energy to provide for the beam driven modes. Moreover, it is a widely accepted fact that the beam velocity can act as a source of free energy which could develop instabilities in the system. The wave energy for an electrostatic wave is

$\epsilon = \omega \frac{\partial D}{\partial \omega} |E|^2$,^{30,31} where $|E|^2$ is the intensity of the wave electric field and $D(\omega, k) = 0$ is the longitudinal dielectric constant of the plasma. The ion acoustic mode has $\epsilon > 0$ as $\frac{\partial D}{\partial \omega}$ is positive, and, thus, it is a positive energy mode.^{30,31} Therefore, to excite this mode, energy needs to be fed into the system, which is provided by the solar wind beam electrons. On the other hand, for the beam driven mode, $\epsilon < 0$ as in this case $\frac{\partial D}{\partial \omega} = \frac{2\omega_{vp}^2}{\omega^3} + \frac{2\omega_{vo}^2}{\omega^3} + \frac{2\omega_{sp}^2}{(\omega - ku_{sp})^3} < 0$, for the input parameters of the plasma system, and it is a negative energy mode.^{30,31} Therefore, to excite this negative energy mode, dissipation is required which is provided mainly by the Venusian electrons. At this point of understanding, we conjecture that the beam driven mode requires the second electron component (i.e., Venusian electrons in this case) when the beam velocity in the system is higher than the phase velocity of the wave $u_{sp} > v_p = \omega_r/k$. Additional studies are required to understand the key tenets of this particular case. To summarize, the low frequency mode is excited with the help of the solar wind beam electrons, whereas the beam driven modes are excited via the solar wind beam protons.

A. Number density of ions variation

In this subsection, the number density of Venusian protons, Venusian oxygen, and solar wind beam proton variation have been carried out. The other fixed normalized plasma parameters are as follows: temperature ratio of the Venusian protons to the solar wind beam electrons and temperature ratio of the Venusian Oxygen to the solar wind beam electrons are $\sigma_{vp} = \sigma_{vo} = 0.003$, temperature ratio of the solar wind protons to the solar wind beam electrons is $\sigma_{sp} = 0.001$, and temperature ratio of the Venusian electrons to the solar wind beam electrons is $\sigma_{ve} = 0.45$. The beam velocity of solar wind protons and electrons is $U_{sp} = U_{se} = 9.84$, and the suprathermal index is $\kappa = 2$. Figure 2(a) shows the effect of the number density of Venusian protons N_{vp} on the ion acoustic mode. It reveals that increase in N_{vp} increases the frequency of the ion acoustic mode. The frequency gap between $N_{vp} = 0.1$ and $N_{vp} = 0.5$ is higher than that of between $N_{vp} = 0.5$ and $N_{vp} = 0.8$. Figure 2(b) shows the variation of N_{vo} on the ion acoustic mode, which also reveals that increase in N_{vo} increases the frequency of the ion acoustic mode. However, the variation from 0.1 to 0.8 for N_{vp} [Fig. 2(a)] shows significant change compared to N_{vo} [Fig. 2(b)]. The frequency of the ion acoustic mode does not change much initially; however, after $k \approx 0.25$, one can witness a slight change in the frequency for different N_{vo} values. We checked the effect of N_{vp} and N_{vo} on the beam driven mode, and there is no noticeable change in the frequency of the beam driven mode. We conclude that the Venusian ions (both proton and oxygen) do not play any role on the beam driven modes. Figure 2(c) shows the effect of the number density of the solar wind beam protons N_{sp} on the real frequency of the ion acoustic mode. The increase in N_{sp} decreases the real frequency of the ion acoustic mode. We have checked the parametric effect of N_{sp} on the beam driven modes; however, we did not see any noticeable change in the real frequency of the beam driven mode for N_{sp} variation.

The instability profile in Fig. 2(d) shows N_{vp} variations on the ion acoustic mode for three parameter sets $N_{vp} = 0.1, 0.5$, and 0.8 . The initial increase in N_{vp} from 0.1 to 0.5 enhances the growth rate of the ion acoustic mode, and further increase in N_{vp} diminishes the growth

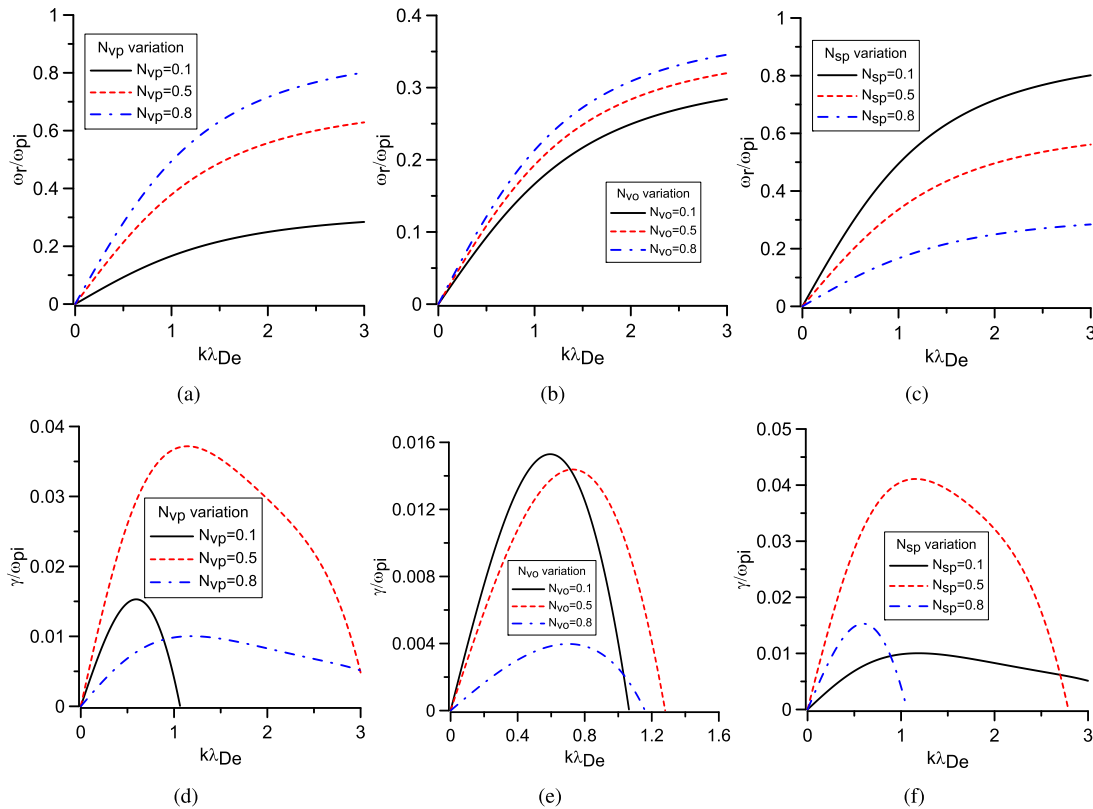


FIG. 2. Dispersion curve variation and its corresponding growth rate variation on the ion acoustic mode: For (a) and (d), we have fixed $N_{vo} = 0.1$; for (b) and (e), we have fixed $N_{vp} = 0.1$; and for (c) and (f), we have fixed $N_{vo} = 0.1$. The remaining number density for each corresponding figure can be obtained from the neutrality condition [Eqs. (14) and (15)]. The other fixed parameters for all figures are $\sigma_{vp} = \sigma_{vo} = 0.003$, $\sigma_{sp} = 0.001$, $\sigma_{ve} = 0.45$, $U_{sp} = U_{se} = 9.84$, and $\kappa = 2$.

rate. The maximum of growth rate for $N_{vp} = 0.1$ is 0.01529 at $k_{\lambda_{De}} = 0.594$, for $N_{vp} = 0.5$ is 0.0372 at $k_{\lambda_{De}} = 1.145$, and for $N_{vp} = 0.8$ is 0.0100 at $k_{\lambda_{De}} = 1.187$. This reveals that maximum of γ has noticeable change with respect to the wavenumber. Contrary to the findings of N_{vp} variation, Fig. 2(e) shows that increase in N_{vo} diminishes the growth rate of the ion acoustic mode. The maximum of growth rate for $N_{vo} = 0.1$ is 0.0153 at $k_{\lambda_{De}} = 0.594$, for $N_{vo} = 0.5$ is 0.01438 at $k_{\lambda_{De}} = 0.728$, and for $N_{vo} = 0.8$ is 0.0039 at $k_{\lambda_{De}} = 0.703$. The initial increase from $N_{vo} = 0.1$ to $N_{vo} = 0.5$ does not alter the instability much, and further increase in N_{vo} significantly lowers the growth rate. The instability profile of N_{sp} is plotted in Fig. 2(f). For $N_{sp} = 0.1$, instability increases and reaches a maximum of 0.01 at $k_{\lambda_{De}} = 1.187$, for $N_{sp} = 0.5$, the maximum is 0.0411 at $k_{\lambda_{De}} = 1.156$, and for $N_{sp} = 0.8$, the maximum is 0.01529 at $k_{\lambda_{De}} = 0.594$. Similar to N_{vp} variation, the maximum of growth rate changes with respect to the wavenumber.

For the case of N_{se} , we have mentioned earlier that whenever the number density of solar wind beam electrons N_{se} or beam velocity of solar wind electrons U_{se} is zero, the low frequency ion acoustic mode excitation is no more possible. We have used the charge neutrality condition [Eq. (14)] for the solar wind components, i.e., $N_{sp} = N_{se}$, so the variation of N_{sp} altering the frequency and the growth rate of the ion acoustic mode in Figs. 2(c) and 2(f) arises from the effect of N_{se} . Since we have used the same number density, the effect of N_{se} and N_{sp} on the ion acoustic mode is essentially the same.

B. Temperature ratio variation

In this subsection, we have explored the impact of temperature ratio variation on the instability. The normalized plasma parameters considered are as follows: number density of the Venusian protons and the Venusian oxygen is $N_{vp} = 0.4$ and $N_{vo} = 0.5$, respectively, number density of the solar wind beam protons and the electrons is $N_{sp} = N_{se} = 0.1$, and the number density of the Venusian electrons is $N_{ve} = 0.9$. The beam velocity of solar wind protons and electrons is $U_{sp} = U_{se} = 9.84$, and the suprathermal index is $\kappa = 2$. Since the temperature ratio of the ions is not present in the real part of the dispersion relation [Eq. (9)], there is no change in the real frequency of any mode with respect to the temperature ratio of ions. Figure 3(a) shows the growth rate variation of the ion acoustic wave mode for three different σ_{vp} values. The instability profile reveals that increase in σ_{vp} decreases the range of wave numbers for which instability is excited. The maximum of γ shifts toward lower k value with increasing σ_{vp} . We explored the effect of σ_{vo} variation on the instability of the ion acoustic mode. The result is in line with the σ_{vp} variation. Increase in σ_{vo} decreases the instability. We have checked the effect of σ_{sp} on the ion acoustic mode, and there is no change in the growth rate of the ion acoustic mode as expected. As we have established from our mode driven analysis that the solar wind beam protons are responsible for the beam driven modes, i.e., σ_{sp} variation would alter only the beam driven

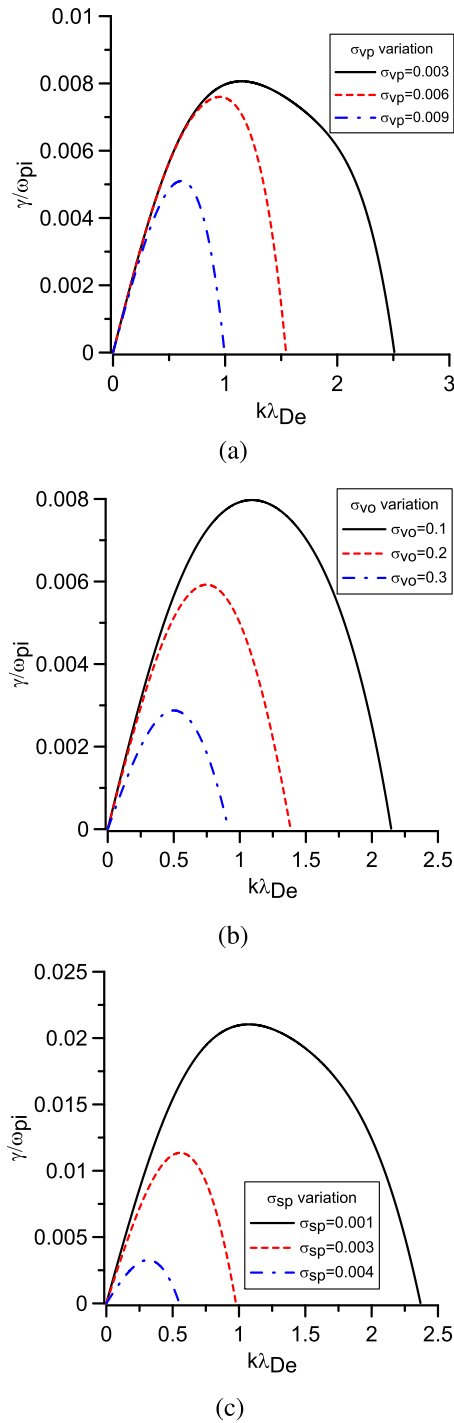


FIG. 3. Effect of different temperature ratios on growth rate: (a) σ_{vp} variation on ion acoustic mode's growth rate, (b) σ_{vo} variation on ion acoustic mode's growth rate, and (c) σ_{sp} variation on beam driven mode's growth rate. The fixed plasma parameters are $N_{vp} = 0.4$, $N_{vo} = 0.5$, $N_{sp} = N_{se} = 0.1$, $N_{ve} = 0.9$, $U_{sp} = U_{se} = 9.84$, and $\kappa = 2$. The values of the temperature ratios are $\sigma_{vp} = \sigma_{vo} = 0.003$, $\sigma_{sp} = 0.001$, and $\sigma_{ve} = 0.45$. For (a), we have varied σ_{vp} while keeping the other temperature ratios fixed. The similar technique was employed for (b) and (c).

mode. Figure 3(c) shows the σ_{sp} variation on beam driven mode. It reveals that increase in σ_{sp} decreases the instability. The maximum of the growth rate is shifting toward the higher value of k with increase in σ_{sp} . Overall, the findings related to the temperature ratio of ions support the notion that for the ion acoustic wave, temperature of the ions does not influence the dispersion relation much. Meanwhile, a popular and an accepted notion is that temperature of electrons plays a crucial role in the dispersion relation of the ion acoustic waves. In order to determine whether it holds good for our model, we have plotted the σ_{ve} variation in Figs. 4(a)–4(c). Our results tie well with the accepted notion wherein the temperature of electrons, indeed, found to impact the dispersion relation,³² the instability of the ion acoustic wave mode, and the instability of the beam driven mode. The instability profile in Fig. 4(b) shows that increase in σ_{ve} enhances the instability of the ion acoustic mode but decreases the instability of the beam driven mode [Fig. 4(c)]. Broadly translated, our findings indicate that the temperature of ions does not affect the wave modes much, whereas the temperature of electrons plays a vital role in both the dispersion relation and the instability of the ion acoustic wave mode.

C. Beam velocity and suprathermal index variation

In this subsection, we have explored the effect of the beam velocity and the suprathermal index variation on the wave modes in our plasma system. The normalized plasma parameters used are as follows: the number density of the Venusian protons and the Venusian Oxygen is $N_{vp} = 0.4$ and $N_{vo} = 0.5$, respectively, the number density of the solar wind beam protons and the electrons is $N_{sp} = N_{se} = 0.1$, and the number density of the Venusian electrons is $N_{ve} = 0.9$. The temperature ratio of the Venusian protons to the solar wind beam electrons and the temperature ratio of the Venusian Oxygen to the solar wind beam electrons are $\sigma_{vp} = \sigma_{vo} = 0.003$, the temperature ratio of the solar wind protons to solar wind beam electrons is $\sigma_{sp} = 0.001$, and the temperature ratio of the Venusian electrons to the solar wind beam electrons is $\sigma_{ve} = 0.45$. Figure 5(a) shows the dispersion relation of solar wind beam velocity variation on the beam driven mode. From the results, it is clear that increase in U_{sp} increases the frequency of the beam driven modes. The instability profile in Fig. 5(b) shows that increase in U_{sp} enhances the instability of the beam driven mode. There is no change in the instability of the ion acoustic mode with respect to U_{sp} variation. As discussed, this is due to the fact that the solar wind beam protons are responsible for only the beam driven modes. Therefore, it did not impact the ion acoustic mode. For the case of U_{se} , the real part of the dispersion relation [Eq. (9)] does not have U_{se} term in the dispersion relation, and, thus, U_{se} does not change the dispersion of the IAW mode (also any wave mode), but it changes the growth rate of the IAW mode. The instability profile in Figs. 5(c) and 5(d) shows the suprathermal index κ variation on the ion acoustic and the beam driven mode. The curves in Fig. 5(c) represent the ion acoustic mode variation, which shows that increase in κ decreases the instability of the ion acoustic mode. The curves in Fig. 5(d) correspond to the beam driven mode variation, which shows that increase in κ increases the instability of the beam driven mode.

IV. CONCLUSION

To summarize, we have studied the role of each species on the instability in an unmagnetized plasma system comprising of Venusian

02 August 2023 11:36:45

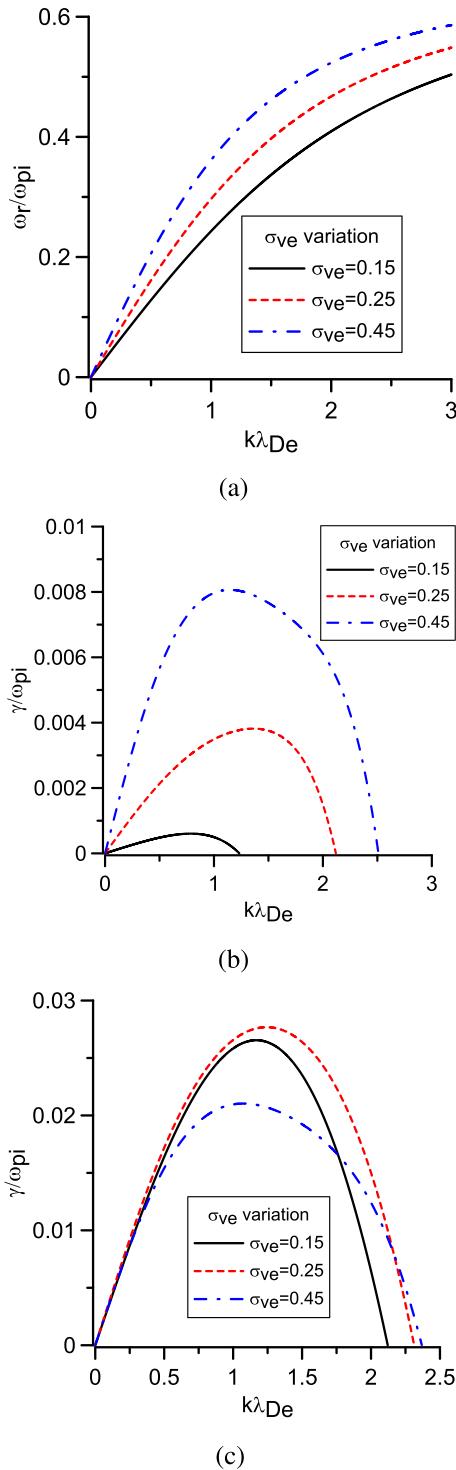


FIG. 4. (a) Effect of σ_{ve} on real frequency of the ion acoustic mode, (b) σ_{ve} variation on the growth rate of the ion acoustic mode, and (c) σ_{ve} variation on the growth rate of the beam driven mode. The fixed plasma parameters are $N_{vp} = 0.4$, $N_{vo} = 0.5$, $N_{sp} = N_{so} = 0.1$, $N_{ve} = 0.9$, $\sigma_{vp} = \sigma_{vo} = 0.003$, $\sigma_{sp} = 0.001$, $U_{sp} = U_{so} = 9.84$, and $\kappa = 2$.

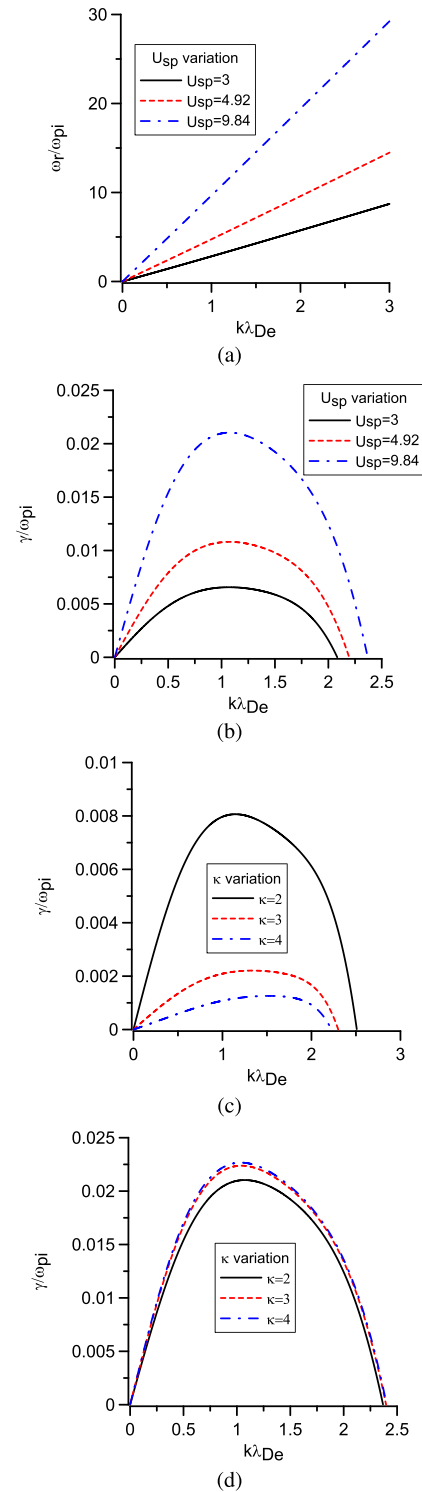


FIG. 5. Real frequency (a) and growth rate (b) variation of beam driven mode. (c) and (d) The growth rate variation of ion acoustic mode and beam driven modes, respectively. The fixed parameters are as follows: $N_{vp} = 0.4$, $N_{vo} = 0.5$, $N_{sp} = N_{so} = 0.1$, $N_{ve} = 0.9$, $\sigma_{vp} = \sigma_{vo} = 0.003$, $\sigma_{sp} = 0.001$, and $\sigma_{ve} = 0.45$.

02 August 2023 11:36:45

protons, Venusian oxygen, solar wind beam protons, and electrons and Venusian electrons. The plasma parameters for this study have been obtained from Lundin *et al.*¹⁷ for the dawn dusk meridian of Venus Express (VEX) with the data from the ASPERA-4 Ion Mass Analyzer (IMA). The detailed mode analysis led to the following conclusions: one low frequency typical ion acoustic wave mode and two high frequency beam driven modes are present in the system. We have obtained the growth for the ion acoustic mode and one of the high frequency beam driven modes. The other high frequency mode is the damped mode and is not discussed here. For Fig. 1, we have found out the unnormalized values corresponding to the maximum growth rate. For the ion acoustic mode in Fig. 1(a), maximum growth $\gamma/\omega_{pi} = 0.0081$ [Fig. 1(c)] occurs at $k\lambda_{De} = 1.145$, and the corresponding real frequency is $\omega/\omega_{pi} = 0.39$. The unnormalized frequency and the unnormalized growth rate are $\omega_{ia}/2\pi = 0.83$ and $\gamma_{ia}/2\pi = 0.0067$ kHz, respectively, and the corresponding wave number is 0.37 m^{-1} . The phase velocity of the ion acoustic mode is $v_{ia} = 2.24 \text{ km/s}$. The beam mode in Fig. 1(b) reaches its maximum growth $\gamma/\omega_{pi} = 0.02$ [Fig. 1(d)] at $k\lambda_{De} = 1.073$, and the corresponding real frequency is $\omega/\omega_{pi} = 10.37$. The unnormalized frequency and the unnormalized growth rate are $\omega_{bm}/2\pi = 21.74$ and $\gamma_{bm}/2\pi = 0.46$ kHz, respectively, and the corresponding wave number is 0.35 m^{-1} . The phase velocity of the beam driven mode is $v_{bm} = 62.53 \text{ km/s}$. For Fig. 1, the unnormalized frequency, growth rate, and phase velocities values for $k = 0.0006 \text{ m}^{-1}$ ($k\lambda_{De} = 0.002$) and ion acoustic and beam mode are $\omega_{ia}/2\pi = 1.81$, $\omega_{bm}/2\pi = 40.36$, $\gamma_{ia}/2\pi = 0.05$, and $\gamma_{bm}/2\pi = 0.15$ Hz, $v_{ia} = 2.8$ and $v_{bm} = 62.28 \text{ km/s}$, respectively. The low frequency ion acoustic wave mode arises in the system from the combination of the Venusian ions' contribution but its wave growth is highly influenced by the solar wind electrons. Meanwhile, solar wind beam protons are responsible for the generation of the high frequency beam driven modes, and we have deduced that wave growth of the beam driven mode is affected by the solar wind beam protons. Extensive parametric investigation revealed that number density of the Venusian ions affects only the ion acoustic mode's frequency and its instability. Similarly, number density of the solar wind beam protons impacts only the beam driven mode. However, when it comes to temperature ratio, our findings indicate that the temperature of ions does not affect the wave modes much, whereas the temperature of electrons plays a vital role in both the dispersion relation and the instability of the ion acoustic wave mode. The beam velocity of the solar wind protons is found to be enhancing both the frequency and the instability of the beam driven mode. Result of suprathermal index variation revealed that increase in κ increases the instability of the beam driven mode but decreases the instability of the ion acoustic mode. We have checked the wave mode analysis and the parametric investigation for other parameters listed in Table I and obtained the similar qualitative results. We have checked the frequency and the wave growth rate for both the ion acoustic and the beam driven modes with respect to altitude variation (Table I). We have used the temperature ratios and the beam velocities mentioned in Fig. 1 for this altitude variation analysis. We have found that when we move up in altitude, the wave growth for the ion acoustic and the beam driven mode increases, indicating that it is more probable to find these wave modes in higher altitude. The frequency of the beam driven mode decreases when altitude increases, and the k value at which the maximum growth rate observed increases with altitude. For the ion acoustic mode, the frequency and the k value

at which the maximum growth rate observed increase initially with altitude and decrease later with respect to altitude. We conjecture that the ion acoustic mode and the beam driven mode may be relevant in explaining the electrostatic noise in the Venusian ionosphere in the range of several hundreds Hz to 1 kHz and several tens kHz, respectively.

ACKNOWLEDGMENTS

This work was carried out by T. Kamalam during her research associateship at the Indian Institute of Geomagnetism. G.S. Lakhina acknowledges the Indian National Science Academy, New Delhi, for the support under the INSA-Honorary Scientist Scheme.

AUTHOR DECLARATIONS

Conflict of Interest

The authors have no conflicts to disclose.

Author Contributions

T. Kamalam: Conceptualization (equal); Formal analysis (equal); Methodology (equal); Software (equal); Validation (equal); Writing – original draft (equal). **Satyavir Singh:** Conceptualization (equal); Methodology (equal); Supervision (lead); Validation (equal); Writing – review & editing (equal). **T. Sreeraj:** Formal analysis (equal); Software (equal); Writing – review & editing (equal). **Gurbax S. Lakhina:** Conceptualization (equal); Supervision (supporting); Validation (equal); Writing – review & editing (equal).

DATA AVAILABILITY

The data that support the findings of this study are available within the article.

REFERENCES

- ¹V. K. Yadav, "Plasma waves around Venus and Mars," *IETE Tech. Rev.* **38**, 622–661 (2020).
- ²D. Müller, O. C. S. Cyr, I. Zouganelis, H. R. Gilbert, R. Marsden, T. Nieves-Chinchilla, E. Antonucci, F. Auchère, D. Berghmans, T. S. Horbury, R. A. Howard, S. Krucker, M. Maksimovic, C. J. Owen, P. Rochus, J. Rodriguez-Pacheco, M. Romoli, S. K. Solanki, R. Bruno, M. Carlsson, A. Fludra, L. Harra, D. M. Hassler, S. Livi, P. Louarn, H. Peter, U. Schühle, L. Teriaca, J. C. del Toro Iniesta, R. F. Wimmer-Schweingruber, E. Marsch, M. Velli, A. D. Groof, A. Walsh, and D. Williams, "The solar orbiter mission," *Astron. Astrophys.* **642**, A1 (2020).
- ³N. J. Fox, M. C. Velli, S. D. Bale, R. Decker, A. Driesman, R. A. Howard, J. C. Kasper, J. Kinnison, M. Kusterer, D. Lario, M. K. Lockwood, D. J. McComas, N. E. Raouafi, and A. Szabo, "The solar probe plus mission: Humanity's first visit to our star," *Space Sci. Rev.* **204**, 7–48 (2015).
- ⁴L. Colin, "The pioneer Venus program," *J. Geophys. Res.* **85**, 7575, <https://doi.org/10.1029/JA085iA13p07575> (1980).
- ⁵J. D. Huba, "Generation of waves in the Venus mantle by the ion acoustic beam instability," *Geophys. Res. Lett.* **20**, 1751–1754, <https://doi.org/10.1029/93GL01984> (1993).
- ⁶C. M. Ho, R. J. Strangeway, and C. T. Russell, "Evidence for langmuir oscillations and a low density cavity in the Venus magnetotail," *Geophys. Res. Lett.* **20**, 2775–2778, <https://doi.org/10.1029/93GL03379> (1993).
- ⁷J. T. M. Daniels, C. T. Russell, R. J. Strangeway, H. Y. Wei, and T. L. Zhang, "Whistler mode bursts in the Venus ionosphere due to lightning: Statistical properties using Venus express magnetometer observations," *J. Geophys. Res.* **117**, E04004, <https://doi.org/10.1029/2011JE003897> (2012).

- ⁸F. L. Scarf, W. W. L. Taylor, and I. M. Green, "Plasma waves near Venus: Initial observations," *Science* **203**, 748–750 (1979).
- ⁹M. Delva, T. L. Zhang, M. Volwerk, W. Magnes, C. T. Russell, and H. Y. Wei, "First upstream proton cyclotron wave observations at Venus," *Geophys. Res. Lett.* **35**, L03105, <https://doi.org/10.1029/2007GL032594> (2008).
- ¹⁰M. Volwerk, T. L. Zhang, M. Delva, Z. Vörös, W. Baumjohann, and K.-H. Glassmeier, "First identification of mirror mode waves in Venus's magnetosheath," *Geophys. Res. Lett.* **35**, L12204, <https://doi.org/10.1029/2008GL033621> (2008).
- ¹¹L. Z. Hadid, N. J. T. Edberg, T. Chust, D. Píša, A. P. Dimmock, M. W. Morooka, M. Maksimovic, Y. V. Khotyaintsev, J. Souček, M. Kretzschmar, A. Vecchio, O. L. Contel, A. Retino, R. C. Allen, M. Volwerk, C. M. Fowler, L. Sorriso-Valvo, T. Karlsson, O. Santolík, I. Kolmašová, F. Sahraoui, K. Stergiopoulou, X. Moussas, K. Issautier, R. M. Dewey, M. K. Wolt, O. E. Malandraki, E. P. Kontar, G. G. Howes, S. D. Bale, T. S. Horbury, M. Martinović, A. Vaivads, V. Krasnoselskikh, E. Lorfèvre, D. Plettemeier, M. Steller, Š. Štverák, P. Trávníček, H. O'Brien, V. Evans, V. Angelini, M. C. Velli, and I. Zouganelis, "Solar orbiter's first Venus flyby: Observations from the radio and plasma wave instrument," *Astron. Astrophys.* **656**, A18 (2021).
- ¹²F. L. Scarf, W. W. L. Taylor, C. T. Russell, and R. C. Elphic, "Pioneer Venus plasma wave observations: The solar wind-Venus interaction," *J. Geophys. Res.* **85**, 7599, <https://doi.org/10.1029/JA085iA13p07599> (1980).
- ¹³R. Strangeway, "Plasma waves at Venus," *Space Sci. Rev.* **55**, 275–316 (1991).
- ¹⁴D. S. Intriligator and F. L. Scarf, "Plasma turbulence in the downstream ionosheath of Venus," *Geophys. Res. Lett.* **9**, 1325–1328, <https://doi.org/10.1029/GL009i012p01325> (1982).
- ¹⁵R. C. Whitten, "Thermal structure of the ionosphere of Venus," *J. Geophys. Res.* **74**, 5623–5628, <https://doi.org/10.1029/JA074i024p05623> (1969).
- ¹⁶F. Sayed, A. Turkey, R. Koramy, and W. Moslem, "Nonlinear ion-acoustic waves at Venus ionosphere," *Adv. Space Res.* **66**, 1276–1285 (2020).
- ¹⁷R. Lundin, S. Barabash, Y. Futaana, J.-A. Sauvaud, A. Fedorov, and H. P. de Tejada, "Ion flow and momentum transfer in the Venus plasma environment," *Icarus* **215**, 751–758 (2011).
- ¹⁸A. A. Fayad, I. S. Elkamash, H. Fichtner, M. Lazar, S. K. El-Labany, and W. M. Moslem, "On the propagation of electrostatic wave modes in the inhomogeneous ionospheric plasma of Venus," *Phys. Plasmas* **28**, 082902 (2021).
- ¹⁹W. Moslem, S. Rezk, U. Abdelsalam, and S. El-Labany, "Shocklike soliton because of an impinge of protons and electrons solar particles with Venus ionosphere," *Adv. Space Res.* **61**, 2190–2197 (2018).
- ²⁰S. Salem, W. Moslem, M. Lazar, R. Sabry, R. Tolba, and R. Schlickeiser, "Ionospheric losses of Venus in the solar wind," *Adv. Space Res.* **65**, 129–137 (2020).
- ²¹A. Elmandoh, A. A. Fayad, R. E. Tolba, and W. M. Moslem, "Soliton, blow up, and shock-like ion-acoustic waves in magnetized plasma at Venus' ionosphere," *Indian J. Phys.* **97**(8), 2537–2545 (2023).
- ²²R. Rubia, S. V. Singh, G. S. Lakhina, S. Devanandhan, M. B. Dhanya, and T. Kamalam, "Electrostatic solitary waves in the Venusian ionosphere pervaded by the solar wind: A theoretical perspective," *Astrophys. J.* **950**, 111 (2023).
- ²³D. Summers and R. M. Thorne, "The modified plasma dispersion function," *Phys. Fluids B: Plasma Phys.* **3**, 1835–1847 (1991).
- ²⁴J. E. Borovsky, J. S. Halekas, and P. L. Whittlesey, "The electron structure of the solar wind," *Front. Astron. Space Sci.* **8**, 690005 (2021).
- ²⁵M. Maksimovic, V. Pierrard, and P. Riley, "Ulysses electron distributions fitted with kappa functions," *Geophys. Res. Lett.* **24**, 1151–1154 (1997).
- ²⁶M. N. S. Qureshi, "Solar wind particle distribution function fitted via the generalized kappa distribution function: Cluster observations," *AIP Conf. Proc.* **679**, 489–492 (2003).
- ²⁷S. Singh and G. Lakhina, "Generation of electron-acoustic waves in the magnetosphere," *Planet. Space Sci.* **49**, 107–114 (2001).
- ²⁸B. D. Fried and S. D. Conte, *The Plasma Dispersion Function* (Elsevier, 1961).
- ²⁹G. Livadiotis, "Introduction to special section on origins and properties of kappa distributions: Statistical background and properties of kappa distributions in space plasmas," *J. Geophys. Res.: Space Phys.* **120**, 1607–1619, <https://doi.org/10.1002/2014JA020825> (2015).
- ³⁰R. A. Cairns, "The role of negative energy waves in some instabilities of parallel flows," *J. Fluid Mech.* **92**, 1–14 (1979).
- ³¹C. N. Lashmore-Davies, "Negative energy waves," *J. Plasma Phys.* **71**, 101–109 (2005).
- ³²F. F. Chen, *Introduction to Plasma Physics and Controlled Fusion* (Springer International Publishing, 2016).